NUMERICAL SIMULATION OF REFRACTION-DIFFRACTION OF WAVES CONSIDERING BREAKING-INDUCED CURRENTS

Sung Bum Yoon[1], Jong In Lee[2], Changhoon Lee[3], and Joon Young Park[4]

[1] Assoc. Prof., Dept. of Civil & Environmental Engineering, Hanyang University
[2] Senior Researcher, Water Resources & Environmental Research Division, Korea Institute of Construction Technology
[3] Assist. Prof., Dept. of Civil & Environmental Engineering, Sejong University
[4] Grad. Student, Dept. of Civil & Environmental Engineering, Hanyang University

Abstract: A wide-angle parabolic approximation equation model considering the interaction between wave and current is employed to simulate the deformation of irregular waves over a submerged shoal. It is found that the model gives qualitative agreements with experimental data for the cases of breaking waves around the shoal. Thus, the effect of breaking-induced current on the refraction-diffraction of waves is well understood.

Key Words: irregular waves, refraction, diffraction, breaking induced currents

1. INTRODUCTION

For accurate simulation of waves propagating over a shoal, a numerical model, which can deal with refraction-diffraction of waves, is indispensable. Among various wave models the parabolic approximation equation model (PAEM) is widely employed due to its simple nature of numerical scheme and considerable accuracy of the solution. The PAEM, developed first by Radder (1979) for the monochromatic waves, is continuously improved to include nonlinear effect, bottom friction, wave breaking, and wave-current interaction by a number of researchers. The range of validity of PAEM for wave propagation direction is extended by Booij (1981) and Kirby (1986) to deal with the waves propagating with large angle to the main wave propagation direction.

Recently, the PAEM is employed to simulate the irregular waves with wide-band frequency and directional spectra by virtue of linear superposition of a number of monochromatic component waves. Yoon et al. (2001a, b) conducted comprehensive numerical simulations using PAEM model for the experimental cases of wave deformation over an elliptic shoal performed by Vincent and Briggs (1989) and found that the PAEM model gives reasonably accurate

solutions for non-breaking waves. However, the accuracy of the model degenerates significantly for breaking waves. Yoon et al. analyzed the reason for the accuracy degeneration of conventional wave models and proposed a new mechanism of breaking-induced current acting on the refraction-diffraction of waves over the shoal.

The present study examines the new mechanism proposed by Yoon et al. (2001a, b). A numerical model of parabolic type considering the interaction between waves and currents is employed, and numerical simulations are conducted for the experimental cases of wave deformation with breaking over an elliptic shoal performed by Vincent and Briggs (1989).

2. GOVERNING EQUATIONS

In the present study the REF/DIF S model developed by Kirby and Ozkan (1994) is used for the simulation of irregular waves. The model employs the wide-angle parabolic approximation equation considering wave-current interaction represented by

$$
\begin{aligned}
&(C_{gn}+U)(A_n)_x - 2\Delta_1 V(A_n)_y + i(\overline{k_n} - a_0 k_n)(C_{gn}+U)A_n \\
&+\left\{\frac{\sigma_n}{2}\left(\frac{C_{gn}+U}{\sigma_n}\right)_x - \Delta_1\sigma_n\left(\frac{V}{\sigma_n}\right)_y\right\}A_n \\
&+i\Delta_n'\left[((CC_g)_n - V^2)\left(\frac{A_n}{\sigma_n}\right)_y\right]_y \\
&-i\Delta_1\left\{\left[UV\left(\frac{A_n}{\sigma_n}\right)_y\right]_x + \left[UV\left(\frac{A_n}{\sigma_n}\right)_x\right]_y\right\} + \frac{w_n}{2}A_n + \alpha A_n \\
&+\frac{-b_1}{k_n}\left\{\left[((CC_g)_n - V^2)\left(\frac{A_n}{\sigma_n}\right)_y\right]_{yx} + 2i\left(\sigma_n V\left(\frac{A_n}{\sigma_n}\right)_y\right)_x\right\} \\
&+b_1\beta_n\left\{2i\omega_n U\left(\frac{A_n}{\sigma_n}\right)_x + 2i\sigma_n V\left(\frac{A_n}{\sigma_n}\right)_y\right. \\
&\left.-2UV\left(\frac{A_n}{\sigma_n}\right)_{xy} + \left[((CC_g)_n - V^2)\left(\frac{A_n}{\sigma_n}\right)_y\right]_y\right\} \\
&-\frac{i}{k_n}\{b_1(\omega_n V)_y + 3(\omega_n U)_x\}\left(\frac{A_n}{\sigma_n}\right)_x \\
&-\Delta_2\left\{\omega_n U\left(\frac{A_n}{\sigma_n}\right)_x + \frac{1}{2}\omega_n U_x\left(\frac{A_n}{\sigma_n}\right)\right\} \\
&+ik\omega_n U(a_0 - 1)\left(\frac{A_n}{\sigma_n}\right) = 0
\end{aligned}
\tag{1}
$$

where,

$$
\beta_n = \frac{(k_n)_x}{k_n^2} + \frac{(k_n((CC_g)_n - U^2))_x}{2k_n^2((CC_g)_n - U^2)} \tag{2}
$$

$$
\Delta_1 = a_1 - b_1, \quad \Delta_2 = 1 + 2a_1 - 2b_1, \quad \Delta_n' = a_1 - b_1\frac{\overline{k_n}}{k_n} \tag{3}
$$

In the above equations the subscript n denotes the nth wave component. A_n is the complex amplitude, k_n the wave number, $\overline{k_n}$ the reference wave number given along the wave incidence boundary, C the phase velocity, C_g the group velocity, w_n the dissipation function for bottom friction, and a_0, a_1 and b_1 are the directional correction factors given by

$$
a_0 = 1, \qquad a_1 = -0.75, \qquad b_1 = -0.25 \tag{4}
$$

σ_n is the intrinsic frequency to take into account the Doppler effect due to currents and is determined by the following dispersion relationship:

$$
\sigma_n^2 = (\omega_n - k_n U)^2 = gk_n \tanh k_n D \tag{5}
$$

where ω_n is the absolute frequency, g the gravitational acceleration, and D the total water depth α is the energy dissipation coefficient for wave breaking given by Thornton and Guza (1983) as

$$
\alpha = \frac{3\sqrt{\pi}}{4}\frac{\overline{f}B^3}{\gamma^4 D^5}H_{rms}^5 \tag{6}
$$

where $\overline{f}$ is a representative frequency, and H_{rms} is a root-mean-squared (rms) wave height. B and γ are the empirical coefficients and are chosen to

be 1 and 0.6, respectively, as recommended in Chawla et al. (1998). When the currents are neglected, (1) is reduced to the parabolic approximation equation developed by Kirby (1986).

After the wave field is solved, the radiation stresses can be evaluated by the following equations (Chawla et al., 1998):

$$S_{xx} = \frac{1}{2}\rho g \sum_{n=1}^{N} |A_n|^2 \left\{ \frac{C_{gn}}{C_n}\left(1+\cos^2\theta_n\right) - \frac{1}{2} \right\} \tag{7}$$

$$S_{yy} = \frac{1}{2}\rho g \sum_{n=1}^{N} |A_n|^2 \left\{ \frac{C_{gn}}{C_n}\left(1+\sin^2\theta_n\right) - \frac{1}{2} \right\} \tag{8}$$

$$S_{xy} = \frac{1}{4}\rho g \sum_{n=1}^{N} |A_n|^2 \frac{C_{gn}}{C_n} \sin 2\theta_n \tag{9}$$

where N represents the total number of wave components, and θ_n is the angle of wave propagation. Using the radiation stresses the current field can be calculated by the following modified shallow water equations:

$$\frac{\partial \bar{\eta}}{\partial t} + \frac{\partial P}{\partial x} + \frac{\partial Q}{\partial y} = 0 \tag{10}$$

$$\frac{\partial P}{\partial t} + \frac{\partial (P^2/D)}{\partial x} + \frac{\partial (PQ/D)}{\partial y} + gD\frac{\partial \bar{\eta}}{\partial x} + \frac{1}{\rho}\left(\frac{\partial S_{xx}}{\partial x} + \frac{\partial S_{xy}}{\partial y} \right) + \frac{gn^2}{D^{7/3}} P\sqrt{P^2+Q^2} = 0 \tag{11}$$

$$\frac{\partial Q}{\partial t} + \frac{\partial (PQ/D)}{\partial x} + \frac{\partial (Q^2/D)}{\partial y} + gD\frac{\partial \bar{\eta}}{\partial y} + \frac{1}{\rho}\left(\frac{\partial S_{xy}}{\partial x} + \frac{\partial S_{yy}}{\partial y} \right) + \frac{gn^2}{D^{7/3}} Q\sqrt{P^2+Q^2} = 0 \tag{12}$$

where $\bar{\eta}$ represents the mean free surface displacement measured upwards from still water level. P and Q are the volume fluxes in horizontal dimensions. D (= h + $\bar{\eta}$) is the total water depth, and n is the Manning's roughness coefficient. The horizontal velocity components, U and V, can be obtained using

$$U = P/D, \quad V = Q/D \tag{13}$$

3. HYDRAULIC EXPERIMENTS OF VINCENT AND BRIGGS (1989)

Vincent and Briggs (1989) conducted comprehensive experiments on the deformation of regular and irregular waves over an elliptic shoal. Waves are generated using the directional spectral wave generator (DSWG) in Coastal Engineering Research Center of U.S. Army Corps of Engineers. Fig. 1 shows the experimental setup of Vincent and Briggs (1989).

For the generation of irregular waves, the following directional spectrum is used:

$$E(f,\theta) = S(f)D(\theta) \tag{14}$$

where f and θ denote respectively the frequency and propagation direction of a component wave. $S(f)$ is the TMA shallow-water frequency spectrum (Bouws et al., 1985) and $D(\theta)$ is the wrapped normal spreading function (Borgman, 1984). More details on the experimental set-up and the directional spectrum for wave generation can be found in Vincent and Briggs (1989).

The experiments of Vincent and Briggs are conducted for three kinds of incident waves with different directional spreadings, i.e., unidirectional (U-series), narrow (N-series) and broad (B-series) directional spreadings. For each case of directional spreading, both the band-width of frequency and the nonlinearity are varied. The measured wave heights for each case are compared with those of monochromatic (M-series) waves, which can serve as a reference to show

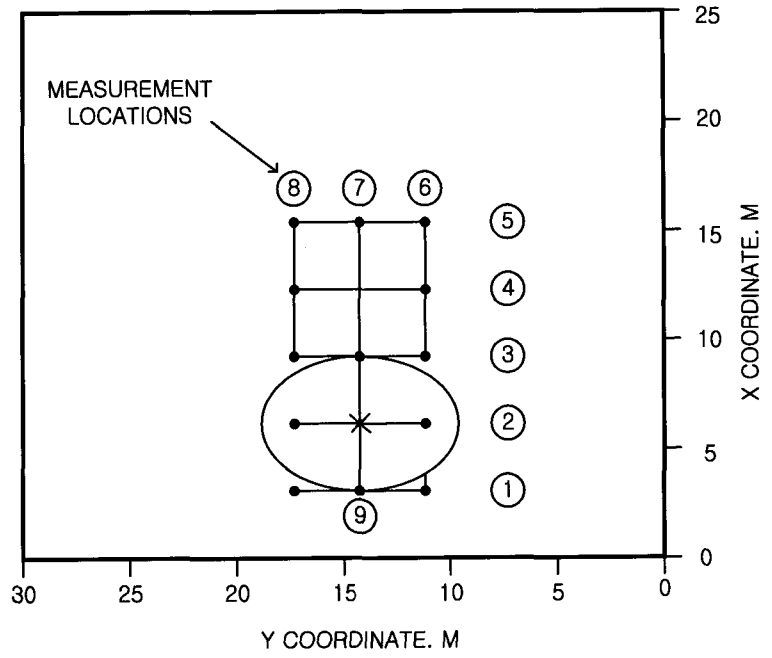

Fig. 1. Location of Elliptic Shoal and Wave Height Measurement Sections (Vincent and Briggs, 1989).

Table 1. Input Wave Conditions for Breaking Waves (Vincent and Briggs, 1989).

Input	Case ID	Peak Period (sec)	Significant Wave Height (cm)	α	γ	σ_m (deg)	Freq. Spreading	Remarks
mono-chromatic	M3	1.3	13.50	-	-	-	mono.	breaking
narrow directional	N5	1.3	19.0	0.0262	20	10	narrow freq.	breaking
broad directional	B5	1.3	19.0	0.0865	2	30	broad freq.	breaking

the effects of frequency and directional spreadings and nonlinearity of incident waves on the wave deformation due to the presence of submerged shoal. Table 1 presents the input wave information for the experimental cases of breaking waves. In the table α, γ and σ_m are the parameters controlling wave height, frequency and directional spreadings of incident wave spectra, respectively, and the details can be found in Vincent and Briggs (1989).

4. NUMERICAL SCHEME

The REF/DIF S model employs the Crank-Nicolson scheme to get the finite difference repressentation of (1). The computational domain (i.e., $0 \le x \le 19$ m, $0 \le y \le 25$ m) is discretized by a finite difference grid with $\Delta x = \Delta y = 0.05$ m. The range of frequency spreading is divided into 10 frequency

components with different value of Δf for each component to have an equal wave energy. The range of directional spreading is divided into 20 directional components. As a result, the irregular waves are disintegrated with a total number of 200 component waves. Each wave component is assumed to be monochromatic with a single frequency and an angle of incidence. Each wave component is calculated independently. However, when the energy dissipation rate is calculated, all the components are superimposed to get *rms* wave heights, H_{rms}.

For the current field (10) – (12) are solved with a finite difference leap-frog scheme on a staggered grid system. The same grid system for wave field is used. The time step of 0.01 seconds is determined by Courant stability condition. Since the current field is symmetric about the centerline of the shoal, only the half domain is solved. The last half of current field can be obtained by mirror image. As a result, the effect of jet meandering on the wave deformation is ignored.

5. TEST OF NUMERICAL MODEL

Yoon et al. (2001a, b) developed a parabolic numerical model similar to REF/DIF S model, but the effect of currents on the deformation of waves was neglected in their model. They tested their model to the experimental cases of Vincent and Briggs (1989). Their model provided reasonably accurate solutions for both monochromatic and irregular waves as long as the waves do not break. However, for the cases of breaking waves the overall pattern of calculated wave height distribution is totally different from the measured one. The inclusion of breaking effect in the computation did not improve the accuracy of the computation as shown in Fig. 2 as an

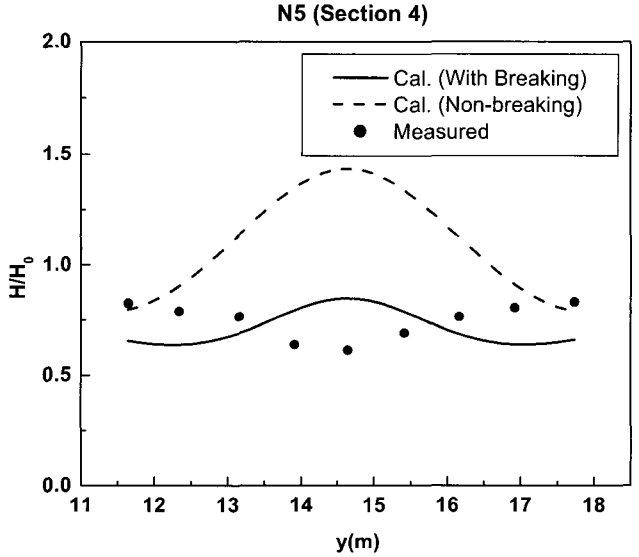

Fig. 2. Comparison of Calculated and Measured Normalized Wave Heights along Section 4 for Case N5 of V-B Experiment; Breaking-induced Currents are Excluded.

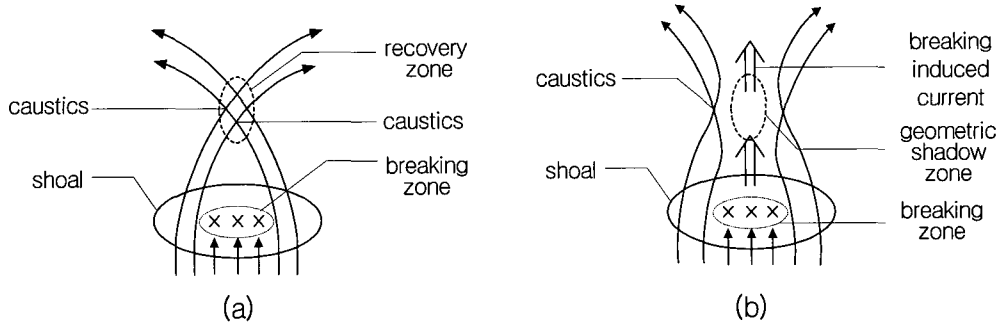

Fig. 3. Schematic Representation of Wave Breaking and Refraction Pattern Over a Shoal ; (a) formation of numerical recovery zone, (b) formation of physical geometric shadow zone.

example. Thus, it was found that the accuracy of the numerical model degenerates significantly for the cases of breaking waves. The interested reader is referred to Yoon et al. (2001a, b) for more details on the performance of the parabolic numerical models.

The accuracy degeneration of numerical model for breaking waves is analyzed by Yoon et al. (2001a, b), and a new mechanism involving the breaking-induced currents is proposed. We repeat briefly their idea here: The breaking of waves over the shoal induces strong currents in the direction of wave propagation as shown in Fig. 3(b), and this breaking-induced currents, in turn, deflects the converging wave rays outwards from the central part behind the shoal. If there is no breaking-induced current, the converging wave rays would form caustics as shown in Fig. 3(a), and the wave height will grow again to form a recovery zone. However, instead of the recovery zone a geometric shadow zone appears there due to deflected wave rays, and two caustics are formed next to the shadow zone. As a result, it may be possible to have a wave height distribution pattern along section 4 consistent with the measured data of Vincent and Briggs (1989). This new mechanism is physically sound and more plausible to explain the discrepancy between the measured and calculated wave climates behind the shoal after the breaking of waves.

6. NUMERICAL SIMULATION CONSIDERING BREAKING-INDUCED CURRENTS

To check the validity of the new concept numerical simulations are conducted for the N5 case of Vincent and Briggs (1989) with considering the breaking-induced current in the computations.

The solution procedure can be summarized here: Firstly, the wave field is calculated using (1) with neglecting the current field, and the radiation stresses are evaluated using (7) - (9). Then, the current field is obtained using (10) - (12). The current field is, in turn, supplied for (1) to get a new wave field. Iterative computations can be made as a transient problem until a steady state is obtained. Strictly speaking, this procedure can be applied only to the steady state problem, because (1) is invalid for a transient wave field.

The breaking-induced current becomes strong as the time elapses, and the wave field is affected

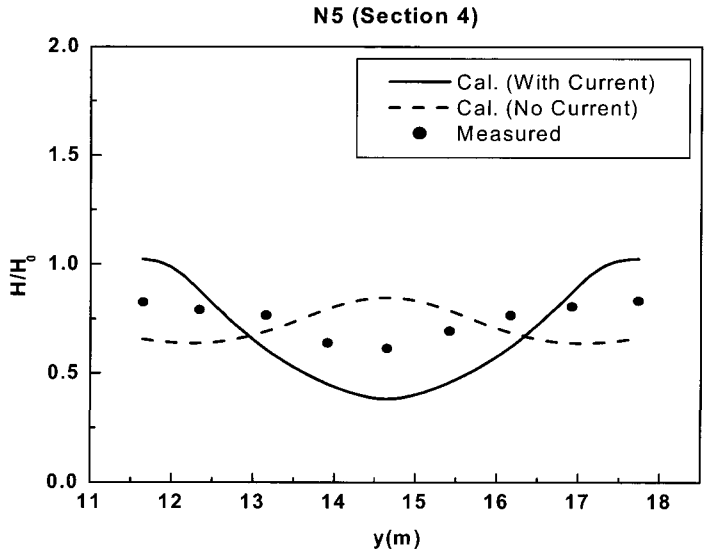

Fig. 4. Comparison of Calculated with Breaking-induced Current and Measured Normalized Wave Heights along Section 4 for Case N5 of V-B Experiment.

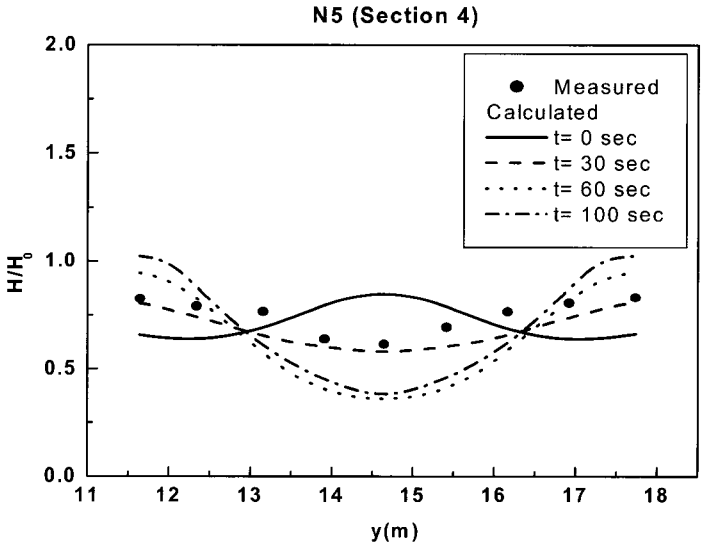

Fig. 5. Evolution of Calculated Normalized Wave Heights along Section 4 for Case N5 of V-B Experiment.

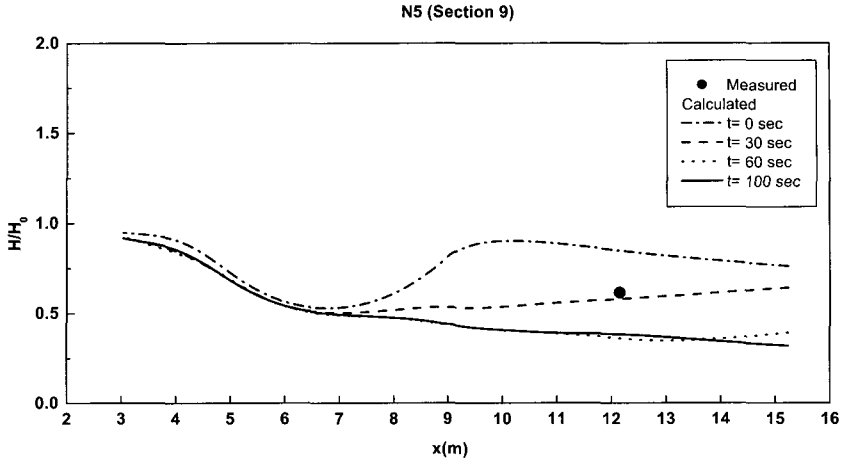

Fig. 6. Evolution of Calculated Normalized Wave Heights along Sections 9 and 7 for Case N5 of V-B Experiment.

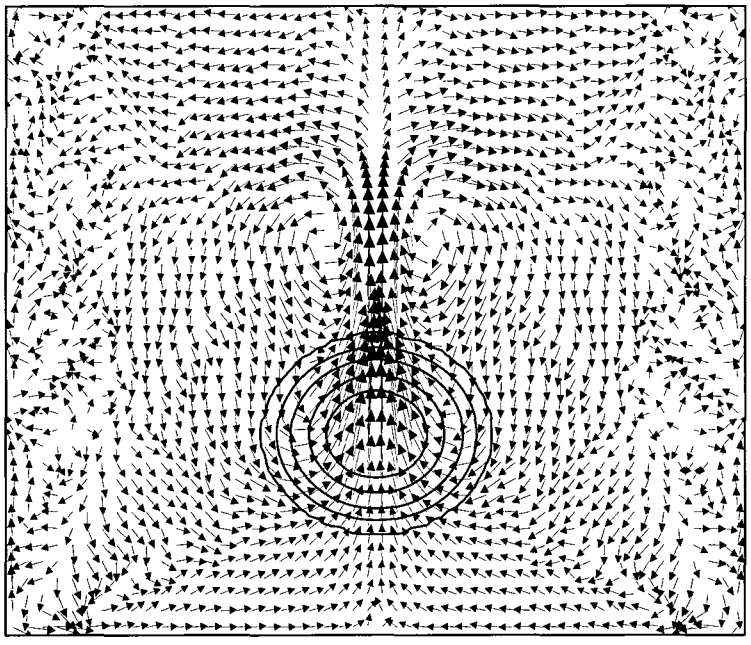

Fig. 7. Flow Pattern of Breaking-induced Currents for Case N5 of V-B Experiment.

by the currents. Thus, at each time step both wave and current fields should be calculated. However, computational experience shows that the evolution of current field is slow. Thus, to save computational time, the wave field is calculated once for 100 time steps of the current field computation. The time step of 0.01 seconds is used for current field computation.

Fig. 4 compares the calculated wave height distributions with measured data along transect 4 for N5 case. All the calculations of wave heights are carried out until the flow field has reached a steady state at transect 4. When the breaking-induced current is included, a qualitative agreement between calculated and measured wave height distributions is observed, while the calculated data with neglecting the current field shows a reversed distribution of wave height. Thus, the effect of breaking- induced current on the refraction-diffraction of waves over the shoal is clearly shown. However, a quantitative agreement is not achieved yet. The reason for this discrepancy may be explained by the two facts: Firstly, the energy dissipation due to wave breaking is possibly over-estimated and the breaking-induced current is stronger than the physical one. In the present study the same parameters for breaking model of Thornton and Guza (1983) is employed as used in REF/DIF S model without any adjustment. Secondly, the wave heights provided by Vincent and Briggs (1989) may be measured before the flow field has reached a steady state. Numerical experience shows that the breaking-induced current evolves slowly such that it takes a considerable time to achieve a steady state around the breaking zone.

Fig. 5 shows the evolution of calculated wave heights along transect 4. At the initial stage the breaking-induced current is absent and the calculated wave height distribution is totally different from the measured one. As time elapses, the current becomes strong. As a result, the wave heights in the central part are reduced, while those of both sides are increased. During the evolution process, a good agreement between calculated and measured wave heights is observed when the time of 30 seconds has elapsed. Fig. 6 presents the evolution of wave height along the centerline of the shoal (i.e., transects 9 and 7 in Fig. 1). It is worthwhile to note here that the wave field reaches a steady state first at the top of the shoal where the breaking of waves are the strongest, and the steady state propagates in downwave direction.

Fig. 7 shows the flow pattern of breaking-induced current field when the current field reached a steady state at section 4. A strong jet along the centerline of the shoal is clearly visible.

7. CONCLUSIONS

To simulate the wave deformation of irregular breaking waves over an elliptic shoal, a system of numerical models is constructed by combining the REF/DIF S model for waves and the flow model for currents. The REF/DIF S model employs the wide-angle parabolic approximation equation considering wave and current interaction. The flow model employs the modified shallow water equations to obtain the current field induced by wave breaking. A numerical test for the experimental case of Vincent and Briggs (1989) shows that the breaking waves induce a jet-like strong current behind the shoal, and the currents, in turn, weaken the focusing of waves. As a result, the distribution patterns of wave height agree much closer to the measured data than those obtained using conventional parabolic numerical models. Thus, the effect of

breaking-induced currents on the refraction-diffraction of waves is well understood.

ACKNOWLEDGEMENTS

This work presented in this paper was surpported by research funds of National Research Labor-atory Program from the Ministry of Science and Technology in Korea (Coastal Engineering Lab-oratory, Hanyang University).

REFERENCES

Booij, N. (1981). *Gravity waves on water with non-uniform depth and current*, Report No. 81-1, Communication on Hydraulics, Department of Civil Engineering, Delft University of Technology, Delft, The Netherlands.

Borgman, L.E. (1984). *Directional spectrum estimation for the Sxy gages.* Technical Report, Coastal Engrg. Res. Center, Vicksburg, p. 104.

Bouws, E., Gunther, H., Rosenthal, W., and Vincent, C.L. (1985). "Similarity of the wind wave spectrum in finite depth water, Part I - Spectral form," *J. Geophysical Res.*, Vol. 90, No. C1, pp. 975-986.

Chawla, A., Ozkan-Haller, H.T., and Kirby, J.T. (1998). "Spectral model for wave transformation and breaking over irregular bathymetry," *J. Waterway, Port, Coastal, and Ocean Engineering,* ASCE, Vol. 124, No. 4, pp. 189-198.

Kirby, J.T. (1986). "Higher-order approximations in the parabolic equation method for water waves." *J. Geophysical Res.*, Vol. 91, No. C1, pp. 933-952.

Kirby, J.T. and Dalrymple, R.A. (1986). "An approximate model for nonlinear dispersion in monochromatic wave propagation models." *Coastal Engineering*, Vol. 9, pp. 78-93.

Kirby, J.T. and Ozkan, H.T. (1994). *Combined refraction/ diffraction model for spectral wave conditions REF/DIF S, version 1.1: Documentation and user's manual.* Center for Applied Coastal Research, Department of Civil Engineering, University of Delaware, Newark, DE19716.

Radder, A.C. (1979). "On the parabolic equation method for water-wave propagation." *J. Fluid Mech.*, Vol. 95, pp. 159-176.

Thornton, E.B. and Guza, R.T. (1983). "Transformation of wave height distribution." *J. Geophys.Res.*, Vol. 88, No. C10, pp. 5925-5938.

Vincent, C.L. and Briggs, M.J. (1989). "Refraction-diffraction of irregular waves over a mound," *J. of Waterway, Port, Coastal, and Ocean Engineering,* ASCE, Vol. 115, No. 2, pp. 269-284.

Yoon, S.B., Lee, J.W., Yeon, Y.J., and Choi, B.H. (2001a). "Numerical simulation of irregular waves over a shoal using parabolic wave model." *J. of Korean Society of Coastal and Ocean Engineers*, Vol. 13, No. 2, pp. 158-168 (in Korean).

Yoon, S.B., Lee, J.W., Yeon, Y.J., and Choi, B.H. (2001b). "A note on the numerical simulation of wave propagation over a submerged shoal." *Proc. of Asian and Pacific Coastal Engineering 2001*, Dalian, China, pp. 315-324.

Sung Bum Yoon, Assoc. Prof., Dept. of Civil & Environmental Engineering, Hanyang University.

(E-mail : sbyoon@email.hanyang.ac.kr)

Jong In Lee, Senior Researcher, Water Resources & Environmental Research Division,

Korea Institute of Construction Technology.
(E-mail : jilee@kict.re.kr)

Changhoon Lee, Assist. Prof., Dept. of Civil & Environmental Engineering, Sejong University
(E-mail : clee@sejong.ac.kr)

Joon Young Park, Grad. Student, Dept. of Civil & Environmental Engineering, Hanyang University
(E-mail : pjyoung73@hanmail.net)